



Optical twists in phase and amplitude

Daria, Vincent R.; Palima, Darwin; Glückstad, Jesper

Published in:
Optics Express

Link to article, DOI:
[10.1364/OE.19.000476](https://doi.org/10.1364/OE.19.000476)

Publication date:
2011

Document Version
Publisher's PDF, also known as Version of record

[Link back to DTU Orbit](#)

Citation (APA):
Daria, V. R., Palima, D., & Glückstad, J. (2011). Optical twists in phase and amplitude. *Optics Express*, 19(2), 476-481. <https://doi.org/10.1364/OE.19.000476>

General rights

Copyright and moral rights for the publications made accessible in the public portal are retained by the authors and/or other copyright owners and it is a condition of accessing publications that users recognise and abide by the legal requirements associated with these rights.

- Users may download and print one copy of any publication from the public portal for the purpose of private study or research.
- You may not further distribute the material or use it for any profit-making activity or commercial gain
- You may freely distribute the URL identifying the publication in the public portal

If you believe that this document breaches copyright please contact us providing details, and we will remove access to the work immediately and investigate your claim.

Optical twists in phase and amplitude

Vincent R. Daria,^{1,*} Darwin Z. Palima,² and Jesper Glückstad^{2,3}

¹ARC Centre for Quantum-Atom Optics, Australian National University, 0200 ACT, Australia

²DTU Fotonik, Dept. of Photonics Engineering, Technical University of Denmark, Denmark

³jesper.gluckstad@fotonik.dtu.dk

*vincent.daria@anu.edu.au

Abstract: Light beams with helical phase profile correspond to photons having orbital angular momentum (OAM). A Laguerre-Gaussian (LG) beam is an example where its helical phase sets a phase-singularity at the optical axis and forms a ring-shaped transverse amplitude profile. Here, we describe a unique beam where both phase and amplitude express a helical profile as the beam propagates in free space. Such a beam can be accurately referred to as an optical twister. We characterize optical twisters and demonstrate their capacity to induce spiral motion on particles trapped along the twisters' path. Unlike LG beams, the far field projection of the twisted optical beam maintains a high photon concentration even at higher values of topological charge. Optical twisters have therefore profound applications to fundamental studies of light and atoms such as in quantum entanglement of the OAM, toroidal traps for cold atoms and for optical manipulation of microscopic particles.

©2011 Optical Society of America

OCIS codes: (350.4855) Optical tweezers or optical manipulation; (260.0260) Physical optics; (350.5500) Propagation; (050.1970) Diffractive optics

References and links

1. L. Allen, M. W. Beijersbergen, R. J. C. Spreeuw, and J. P. Woerdman, "Orbital angular momentum of light and the transformation of Laguerre-Gaussian laser modes," *Phys. Rev. A* **45**(11), 8185–8189 (1992).
2. L. Allen, M. J. Padgett, and M. Babiker, "The orbital angular momentum of light," *Prog. Opt.* **39**, 291–372 (1999).
3. K. P. Marzlin, W. Zhang, and E. Wright, "Vortex coupler for atomic Bose-Einstein condensates," *Phys. Rev. Lett.* **79**(24), 4728–4731 (1997).
4. M. A. Clifford, J. Arlt, J. Courtial, and K. Dholakia, "High-order Laguerre-Gaussian laser modes for studies of cold atoms," *Opt. Commun.* **156**(4-6), 300–306 (1998).
5. M. J. Holland, and J. E. Williams, "Preparing topological states of a Bose-Einstein condensate," *Nature* **401**(6753), 568–572 (1999).
6. M. F. Andersen, C. Ryu, P. Cladé, V. Natarajan, A. Vaziri, K. Helmerson, and W. D. Phillips, "Quantized rotation of atoms from photons with orbital angular momentum," *Phys. Rev. Lett.* **97**(17), 170406 (2006).
7. H. He, M. E. J. Friese, N. R. Heckenberg, and H. Rubinsztein-Dunlop, "Direct observation of transfer of angular momentum to absorptive particles from a laser beam with a phase singularity," *Phys. Rev. Lett.* **75**(5), 826–829 (1995).
8. H. He, N. R. Heckenberg, and H. Rubinsztein-Dunlop, "Optical particle trapping with higher-order doughnut beams produced using high efficiency computer generated holograms," *J. Mod. Opt.* **42**(1), 217–223 (1995).
9. M. E. J. Friese, J. Enger, H. Rubinsztein-Dunlop, and N. R. Heckenberg, "Optical angular-momentum transfer to trapped absorbing particles," *Phys. Rev. A* **54**(2), 1593–1596 (1996).
10. V. Garcés-Chávez, K. Volke-Sepulveda, S. Chavez-Cerda, W. Sibbett, and K. Dholakia, "Transfer of orbital angular momentum to an optically trapped low-index particle," *Phys. Rev. A* **66**(6), 063402 (2002).
11. N. B. Simpson, K. Dholakia, L. Allen, and M. J. Padgett, "Mechanical equivalence of spin and orbital angular momentum of light: an optical spanner," *Opt. Lett.* **22**(1), 52–54 (1997).
12. A. Mair, A. Vaziri, G. Weihs, and A. Zeilinger, "Entanglement of the orbital angular momentum states of photons," *Nature* **412**(6844), 313–316 (2001).
13. S. Franke-Arnold, S. M. Barnett, M. J. Padgett, and M. J. Allen, "Two-photon entanglement of orbital angular momentum states," *Phys. Rev. A* **65**(3), 033823 (2002).
14. C. A. Alonzo, P. J. Rodrigo, and J. Glückstad, "Helico-conical optical beams: a product of helical and conical phase fronts," *Opt. Express* **13**(5), 1749–1760 (2005).
15. G. Overton, "Optical vortices: phase functions are inseparable in Helico-Conical beams," *Laser Focus World*, Optoelectronic world news, May 2005.
16. Y. Schechner, R. Piestun, and J. Shamir, "Wave propagation with rotating intensity distribution," *Phys. Rev. E Stat. Phys. Plasmas Fluids Relat. Interdiscip. Topics* **54**(1), 50–53 (1996).

17. A. S. Desyatnikov, and Y. S. Kivshar, "Rotating optical soliton clusters." *Phys. Rev. Lett.* **88**(5), 053901 (2002).
 18. D. Buccoliero, A. S. Desyatnikov, W. Krolikowski, and Y. S. Kivshar, "Spiraling multivortex solitons in nonlocal nonlinear media," *Opt. Lett.* **33**(2), 198–200 (2008).
 19. V. Jarutis, A. Matijosius, P. Di Trapani, and A. Piskarskas, "Spiraling zero-order Bessel beam," *Opt. Lett.* **34**(14), 2129–2131 (2009).
 20. E. R. Dufresne, and D. G. Grier, "Optical tweezer arrays and optical substrates created with diffractive optics," *Rev. Sci. Instrum.* **69**(5), 1974–1977 (1998).
 21. M. Reicherter, T. Haist, E. U. Wagemann, and H. J. Tiziani, "Optical particle trapping with computer-generated holograms written on a liquid-crystal display," *Opt. Lett.* **24**(9), 608–610 (1999).
 22. J. Goodman, *Introduction to Fourier Optics* (McGraw-Hill 1996).
-

1. Introduction

The unique nature of optical fields with helical phase profile [1,2] have brought about fundamental studies in light-matter interaction ranging from: (1) creating super-fluid vortex modes in Bose-Einstein condensates [3–5]; (2) rotating cold atoms [6]; and (3) revolving microscopic particles [7–11]. These beams are commonly referred to as Laguerre-Gaussian (LG) beams or optical vortices, where the helical phase is expressed by $\exp(-il\phi)$ and l is the topological charge that quantifies the helicity of the wavefront. In quantum theory, l relates to a quantized orbital angular momentum (OAM) of $l\hbar$ per photon [1,2], which forms the basis for experiments on the entanglement of photons [12,13].

From a classical perspective, the helical phase profile of LG beams sets an azimuthal component of the Poynting vector. In the far field, such components interfere to form a dark centre surrounded by a high intensity ring of light. As the topological charge is increased, the dark core at the centre increases and correspondingly enlarging the radius of the light ring. When focused using a lens, the propagation of an LG beam along the optical axis follows a conical ray until it reaches a minimum ring radius and conically increases again after the focal plane. At the focal plane, a high concentration of photons is maintained at the outskirts of the beam forming a ring. From a quantum perspective, one can perceive that the probability of detecting photons with OAM is optimal along the ring of light and negligible at the central dark core.

Increasing the topological charge (and consequently the OAM) of LG beams spreads the distribution of photons around a larger ring. This becomes a problem since increasing topological charge decreases the photon density, which poses some limitations in experiments requiring higher OAM. Various experiments such as in cold atoms and quantum entanglement require high photon densities within a small interaction region. Therefore, the challenge is to produce a beam with scalable OAM while maintaining a high concentration of photons.

Here, we propose a unique beam that has a twisted propagation in both phase and amplitude profile. Such beam can be accurately described as an optical twister where high photon concentrations can be traced along a spiral path but with minimal photon spread even with higher OAM. The optical twister is a special case of a general set of Helico-Conical beams described by us previously [14] and featured in ref. 15. Rotating high-order LG beams have been studied in the past by superposing beams with multiple and non-circularly symmetric phase dislocations about the optical axis [16]. Moreover, Hermite-Laguerre-Gaussian modes or multi-vortex solitons have been reported to rotate as they propagate in non-linear media [17,18]. In contrast to these previous works, the optical twister has a single phase-dislocation along the optical axis with phase and amplitude profile spiraling as the beam propagates in free space. A spiraling zero-order Bessel beam has also been proposed using a spiral phase profile combined with an axicon [19]. Such beam, however, is not known to carry OAM and does not produce a continuous spiraling beam profile since the beam reverses in chirality after the focus. The optical twisters that we describe here maintain chirality as they propagate beyond the focus. Moreover, we show that the optical twisters can introduce spiral motion on particles trapped along their spiral orbit via the transfer of OAM.

2. 3D structure of an optical twister

The optical twister we use here is a subset of Helico-Conical beams introduced and described previously [14]. Figure 1 shows a conceptual overview of the setup. The beam is produced via holographic micro-projection method [8,20,21] where the field of an incident laser is encoded with an appropriate phase pattern at the back focal plane of a Fourier transforming lens. The input field is given by

$$e(\rho, \varphi) = A(\rho) \exp \left[-i \left(l \varphi \frac{\rho}{\rho_o} \right) \right], \quad (1)$$

where ρ is the radial distance from the optical axis, φ is the azimuthal angle and $A(\rho)$ is a circular aperture of radius ρ_o . After the lens, the beam tapers towards a smallest radius at the focus and enlarges after the focus. Hence, the beam has a region of highest concentration of photons at the focus. The incorporation of a conical phase varies the helical phase linearly generating a distinctly different beam as compared to LG and Bessel beams.

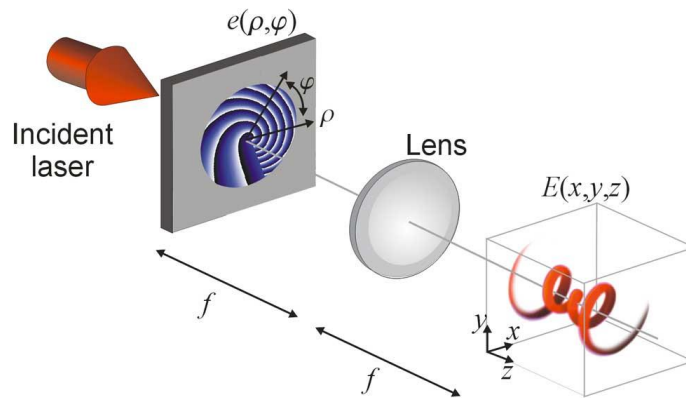


Fig. 1. Conceptual overview of the setup for generating an optical twister.

The three-dimensional (3D) intensity distribution of optical twisters, $I = E^*E$, is difficult to derive analytically due to the fact that the phase at the input has an inseparable dependence between ρ and φ . To visualize the intensity distribution at the output, we numerically evaluate the intensity distribution via the Fresnel diffraction integral [22] which incorporates a lens function of numerical aperture, $NA = 0.2$. From the intensity distribution, we can determine the maximum intensity and also track the radius of the ring for both LG and optical twisters. Figure 2(a) shows the maximum intensities as a function of topological charge for LG and optical twisters. As the topological charge is increased, we expect a decrease in intensity due to an increase in ring radius. The insets in Fig. 2(a) show intensity distributions integrated over several xz -planes (side view). Figure 2(b) shows the radius of the ring for both LG and spiral beams. The rate at which the radius of LG beams increases with topological charge is $6 \times$ higher than spiral beams. Such indicates that majority of the photons are concentrated within a small region around the optical axis. The insets in Fig. 2(b) are intensity distributions integrated over axial several axial or xy -planes (top view). The intensity distributions show that the optical twisters maintain a dark core due to the phase-singularity at the optical axis. Moreover, the region of highest photon density spirals and tapers towards the focal plane. Compared to an LG beam of similar charge, the radius at the focal plane of the optical twister is significantly smaller. The photon density is also significantly higher for the optical twister. The optical twister with $l = 20$ shows a more pronounced twist in the intensity distribution viewed from the side.

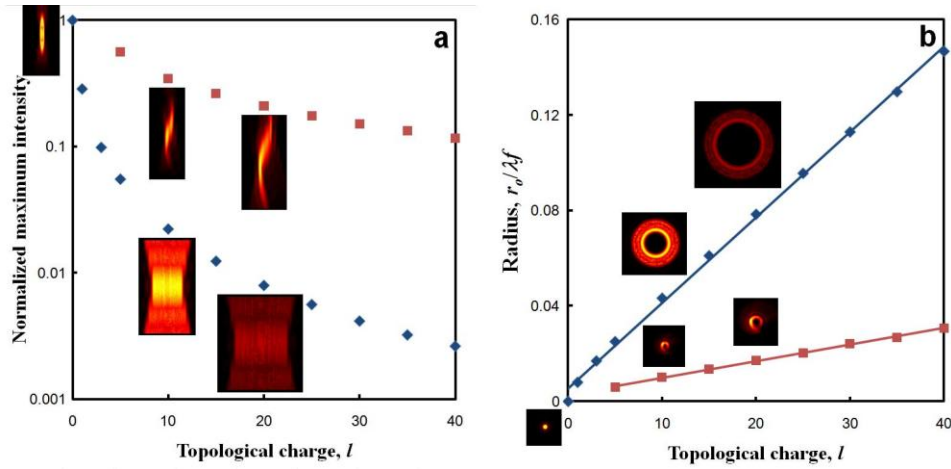


Fig. 2. Characterization plots for spiral (■) and LG beams (◆) showing: (a) Normalized maximum intensity; (b) radius of the ring. The insets show intensity distributions (top and side view) for the Airy function ($l = 0$), Laguerre Gaussian beams and optical twisters for $l = 10$ and $l = 20$.

The region of highest photon concentration and smallest transverse radius points to the effective focal point of the optical twister. The majority of photon concentration is confined within a single helical cycle. Multiple single-cycle twisters can be then generated by holographic splitting of a single incident beam and manipulating the 3D positions via the combination of lens and prism functions and multiplying with the field given by Eq. (1). The effective input field for generating multiple optical twisters is given by

$$e(\rho, \varphi) = A(\rho) \sum_{n=0}^N \exp \left[i \frac{2\pi}{\lambda f} (\rho r_n \cos(\theta_n - \phi) - \rho^2 z_n) - i l \varphi \frac{\rho}{\rho_o} \right], \quad (2)$$

where λ is the wavelength of the incident laser, f is the focal length of the Fourier lens, while $r_n^2 = x_n^2 + y_n^2$, $\theta_n = \tan^{-1}(y_n/x_n)$ and z_n are cylindrical coordinates at the focal volume referring to the position of the n^{th} optical twister. Figure 3 shows intensity distributions of multiple optical twisters visualized along xz -plane. Figure 3(a) shows two ($N = 2$) twisters positioned at $(x_n, y_n, z_n) = (-a, 0, -a)$ and $(+a, 0, +a)$, where a is an arbitrary position. Figure 3(b) also shows two ($N = 2$) twisters aligned along the optical axis forming a chain with $(x_n, y_n, z_n) = (0, 0, +a)$ and $(0, 0, -a)$. Figure 3(c) shows two chains built from four ($N = 4$) twisters with $(x_n, y_n, z_n) = (-a, 0, +a)$, $(-a, 0, -a)$, $(+a, 0, +a)$ and $(+a, 0, -a)$.

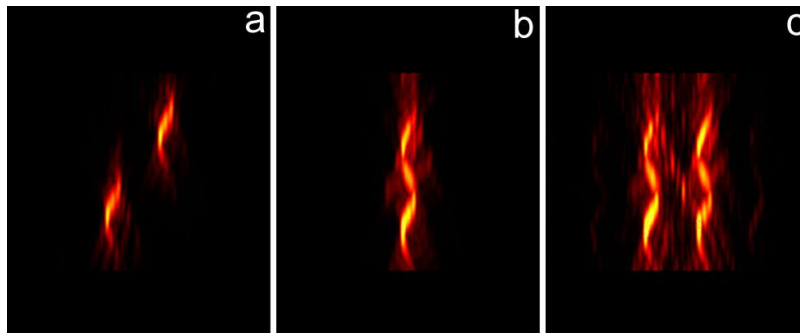


Fig. 3. Multiple optical twisters: (a) disjoint (b) forming a twister-chain (c) multiple chains.

3. Experiment

The optical setup is shown in Fig. 4, which is based on a standard SLM-based optical tweezers setup, where diffractively generated light patterns are demagnified and relayed to a sample through an inverted microscope [7,20,21]. This setup is used to verify the capacity of optical twisters to transfer both linear and orbital angular momentum on microscopic particles. We used a collimated laser source from a continuous wave near infrared (NIR) Ti:S laser (Spectra Physics 3900s) pumped by a Nd:YVO₄ laser (Spectra Physics Millennia 5W). The NIR laser beam ($\lambda \sim 800$ nm) is expanded (via L1 and L2) to illuminate the full area of the spatial light modulator (SLM, Hamamatsu Photonics). The second lens (L2) of the folded beam expander also functions as an optical Fourier transform lens for the phase-encoded reflection from the SLM to form spiral beams at the Fourier plane. Reusing lens L2 minimizes the tilt angle between the incident and phase encoded beam. Minimizing the tilt produces high degree of purity when encoding LG and twister beams. The beams are translated into micron scale at the sample volume using L3 and objective lens arranged in a $4f$ lens configuration. The dichroic mirror reflects the incident NIR and transmits visible light, which carries image information from the sample.

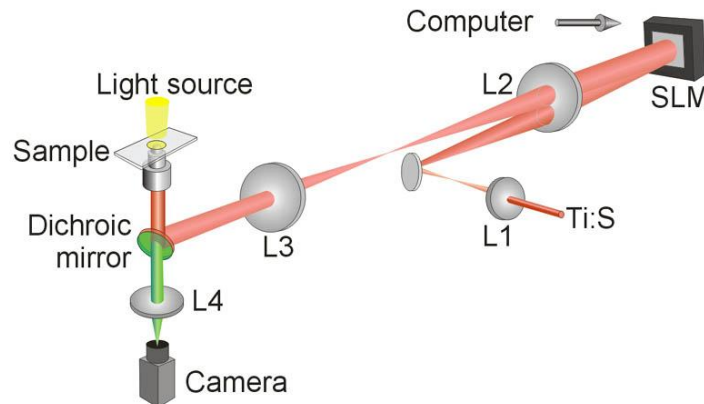


Fig. 4. Optical setup for generating optical twisters and analyzing its capacity to transfer linear and orbital angular momentum on microscopic dielectric particles.

The two-dimensional phase pattern is derived using the phase of Eq. (2). Encoding of the hologram on the SLM is achieved via a secondary video output with 800×600 pixel resolution. A program developed in LabVIEW (National Instruments) enables control of the SLM to encode phase patterns with adjustable topological charge and allows the acquisition of video data from the camera.

To characterize the beam, we verify its capacity to induce linear and orbital angular momentum on particles. Since the intensity of the beam twists as it propagates along the optical axis, we can expect a dielectric particle approaching a spiral beam to be trapped along the region of highest photon density via gradient forces. The beam follows a spiral profile and so particles are expected to be trapped along the orbit and follow a spiral motion with an axial component of the momentum towards the direction of the beam propagation. Moreover, since the beam also has azimuthal component, we also expect that a tangential component of the momentum is transferred to the particle.

To test the transfer of momentum on microscopic dielectric particles, silica beads ($2 \mu\text{m}$ diameter) were dispersed in water and placed in a sample chamber made from microscope cover slips. The bead solution is bounded in a channel, which is around $100 \mu\text{m}$ deep. The optical trapping portion of the experimental setup, described in Fig. 4, uses an inverted microscope (Leica). As such, the beams are directed upwards to allow beads settling at the bottom of the cover slip to be propelled via the spiral beams. Figure 5 shows time lapse images of a particle trapped along the orbit as it approaches the spiral beam with $l = 20$. The

time interval between each frame is 40 ms. With maximum photon density at the focus, majority of the momentum transfer occurs at this region sending the particle into a spiral motion. Previous works have demonstrated a particle trapped along a ring of a LG beam via gradient forces [9,10]. The trapped particle, typically pushed by radiation pressure against the wall of the sample chamber, revolves around the doughnut beam with continuous transfer of OAM. However, without the bounding wall, a particle passing through the LG beam will not follow a helical path and, instead, will be deflected only at the plane of highest intensity due to instantaneous transfer of OAM. Here, we show a unique case where the particle follows a helical path as it exits the optical twister. When the particles enter the optical twister and within the region of highest photon density, both linear and orbital angular momentum gets transferred to the particle, which then undergoes helical motion as it exits the twister.

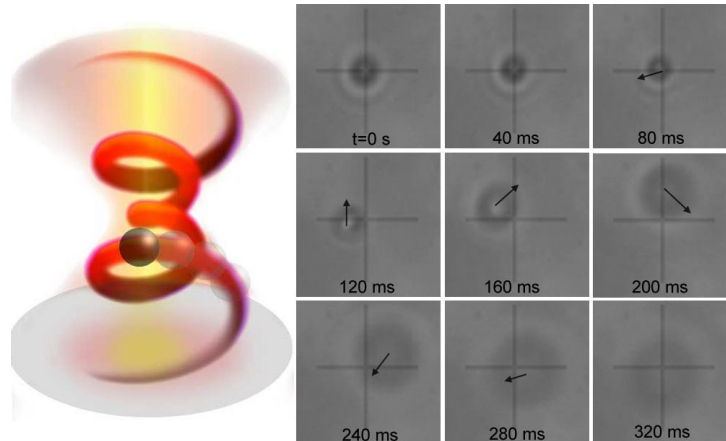


Fig. 5. (Media 1) Time lapse images of a microbead trapped and guided along the orbit of an optical twister. Radiation pressure propels the particle towards the direction of the beam. However, the particle follows the spiral motion via the transfer of orbital angular momentum. Illustration on the left describes the motion of a particle in an optical twister.

4. Conclusions

We have described a diffracting beam with a spiral profile on both the amplitude and phase of the beam. The three dimensional beam structure at the focal region shows an intensity distribution that can be accurately described as an “optical twister” as it propagates in the forward direction. In contrast to LG beams, optical twisters maintain a high concentration of photons at the focus even as the topological charge is increased. Multiple optical twisters and twister chains can also be generated via holographic projection. Finally, we have shown that the optical twisters induce spiral motion on particles trapped along its helical orbit. Optical twisters can have direct application to fundamental studies of light and atoms such as in quantum entanglement of the OAM, toroidal traps for cold atoms and for optical manipulation of microscopic particles.

Acknowledgements

This collaborative work has been made possible via the Short Term Scientific Mission of the COST Action MP0604 and the Australian Academy of Science. V.R.D. has been funded partially by the Australian National University – Office of the Vice-Chancellor. D.P. and J.G. acknowledge financial support from the Danish Technical Scientific Research Council (FTP). We also thank P.J. Rodrigo for discussions and experimental assistance.